

The Crack Growth Behavior in electrolyte membrane under Mechanical-electrochemical Loading

Yun J Chen¹, Yi Sun^{1,*}, Yi Z Liu¹, Chen Wang¹

¹ Department of Astronautic Science and Mechanics, Harbin Institute of Technology, Harbin 150001, PR China

* Corresponding author: sunyi@hit.edu.cn

Abstract As the key component of SOFC (solid oxide fuel cell), a theoretical framework has been built to illustrate the coupling effect between oxygen vacancy concentration and stress field in early works. Here, the coupling theory is expanded and more affecting factors are taken into consideration. An electrolyte membrane with a macro crack is studied by a modified multi-scale method under fully coupling effect. It can be observed that the crack propagates with the increase of remote loadings, and the fracture mode is brittle fracture. The local stress concentration at the crack tip influences significantly the electromechanical fields and the fracture toughness of the stoichiometric sample ($\text{Ce}_{0.8}\text{Gd}_{0.2}\text{O}_{1.9}$) may be reduced from $0.9493\text{MPa}\cdot\text{m}^{1/2}$ of uncoupled value to $0.5142\text{MPa}\cdot\text{m}^{1/2}$. It can be concluded that the coupling effect is important for the electrolyte in the working environment; especially in the case of the existence of a crack.

Keywords: electrolyte membrane, mechanical-electrochemical coupling, multi-scale simulation, fracture toughness

1. Introduction

As an energy conversion device, solid oxide fuel cell (SOFC) can generate high efficiency electric power without environment pollution^[1], and it has attracted more and more attention for its excellent property. Meanwhile, as the core component, considerable researches have been completed to study the performance of the electrolyte^[2].

The GDC (Gadolinium (Gd_2O_3) doped ceria (CeO_2)) is regarded as a promising candidate electrolyte material for its higher ionic conductivity^[3]. When two cerium ions (Ce^{4+}) are replaced by gadolinium ions (Gd^{3+}), an oxygen vacancy is generated to maintain electrical neutrality. And oxygen ions can transport through the electrolyte at high temperature. In the working environment, the effects of temperature and stress are inevitable, the electrolyte actually works in a complicated coupling field^[4-6].

In the present work, a modified multi-scale method is introduced and applied to simulate the electrolyte with a crack under the full coupling effect. Based on the simulation results, the reasons and the process of the electrolyte failure can be further revealed.

2. Framework of the coupling effect

2.1. The stress-induced diffusion potential

When the electrolyte (GDC) is at low oxygen partial pressure, extra oxygen vacancies are generated owing to reduction reaction, and the elastic constants of the material can be assumed a function of the vacancy concentration:

$$C_{ijkl} = C_{ijkl}^0 + \sum_{\alpha} \left(\frac{\partial C_{ijkl}}{\partial \rho_{\alpha}} \right) \Big|_{\rho=\rho_{\alpha}} d\rho_{\alpha} \quad (1)$$

where, ρ_α is the molar fraction of defect α , and C_{ijkl}^0 is the elastic constant of stoichiometric material ($\rho_\alpha = \rho_\alpha^0$). For isotropic material, there are only two independent parameters: E, ν .

$$C_{ijkl} = E\nu / ((1+\nu)(1-2\nu)) \delta_{ij} \delta_{kl} + E / (2(1+\nu)) (\delta_{ik} \delta_{jl} + \delta_{il} \delta_{jk}) \quad (2)$$

Here, η_α , $\eta_{E\alpha}$ and $\eta_{\nu\alpha}$ are introduced for convenience:

$$\eta_\alpha = dV / (3V^0 d\rho_\alpha), \eta_{E\alpha} = dE / (E^0 d\rho_\alpha), \eta_{\nu\alpha} = d\nu / (\nu^0 d\rho_\alpha) \quad (3)$$

where, V^0 , E^0 and ν^0 are volume, Young's modulus and Poisson's ratio of the stoichiometric material. The real Young's modulus and Poisson's ratio are:

$$E = E^0 \left(1 + \sum_\alpha \eta_{E\alpha} \Delta\rho_\alpha \right) \quad (4)$$

$$\nu = \nu^0 \left(1 + \sum_\alpha \eta_{\nu\alpha} \Delta\rho_\alpha \right) \quad (5)$$

In the next, $\sum \eta$, $\sum E$ and $\sum \nu$ are introduced to represent $\sum_\alpha \eta_\alpha \Delta\rho_\alpha$, $\sum_\alpha \eta_{E\alpha} \Delta\rho_\alpha$ and $\sum_\alpha \eta_{\nu\alpha} \Delta\rho_\alpha$.

By using these symbols, formula (2) can be rewritten as:

$$C_{ijkl} = C_{ijkl}^0 \left(1 + \sum E - \frac{\nu^0}{1+\nu^0} \sum \nu \right) + \frac{E^0 \nu^0}{(1+\nu^0)(1-2\nu^0)^2} (\sum \nu) (\delta_{ij} \delta_{kl}) \quad (6)$$

where

$$C_{ijkl}^0 = E^0 \nu^0 / ((1+\nu^0)(1-2\nu^0)) \delta_{ij} \delta_{kl} + E^0 / (2(1+\nu^0)) (\delta_{ik} \delta_{jl} + \delta_{il} \delta_{jk}) \quad (7)$$

Based on formula (6), the constitutive relation can be defined:

$$\begin{aligned} \sigma_{ij} &= C_{ijkl} \varepsilon_{kl}^E = C_{ijkl} (\varepsilon_{kl} - \varepsilon_{kl}^*) \\ &= K^0 \left(1 + \sum E - \frac{\nu^0}{1+\nu^0} \sum \nu \right) \left[\nu^0 \varepsilon_{kk} \delta_{ij} + (1-2\nu^0) \varepsilon_{ij} - (1+\nu^0) \sum \eta \delta_{ij} \right] \\ &\quad + \frac{K^0 \nu^0}{1-2\nu^0} (\sum \nu) (\varepsilon_{kk} - \sum \eta) \delta_{ij} \end{aligned} \quad (8)$$

where $\varepsilon_{ij}^* = \sum_\alpha \eta_\alpha \Delta\rho_\alpha \delta_{ij}$ is the eigenstrain caused by non-stoichiometry effect, η_α is called

coefficient of compositional expansion (CCE), and $K^0 = E^0 / ((1+\nu^0)(1-2\nu^0))$.

The full diffusion potential for isotropic material can be described^[7-8]:

$$\begin{aligned} \tau_\alpha &= \frac{1+3\sum \eta}{2} \left\{ \frac{\nu^0}{E^0} (\eta_{\nu\alpha} - \eta_{E\alpha}) (\sigma_{kk})^2 + \frac{1+\nu^0}{E^0} \left(\eta_{E\alpha} - \frac{\nu^0}{1+\nu^0} \eta_{\nu\alpha} \right) \sigma_{ij} \sigma_{ij} \right\} \\ &\quad + \eta_\alpha \left\{ -\frac{3\nu^0}{2E^0} (\sigma_{kk})^2 + \frac{3(1+\nu^0)}{2E^0} \sigma_{ij} \sigma_{ij} - \sigma_{kk} \right\} \end{aligned} \quad (9)$$

Because the Poisson's ratio has less affected by oxygen vacancy, η_v can be set zero. Once τ_v is obtained, it can be plugged into diffusion and mechanical equations^[8]. The distribution of oxygen vacancy and stress field under coupling effect can be calculated.

In the present work, the electrolyte is $\text{Ce}_{0.8}\text{Gd}_{0.2}\text{O}_{1.9}$ (20GDC), the corresponding non-stoichiometry chemical formula is $\text{Ce}_{0.8}\text{Gd}_{0.2}\text{O}_{1.9-\delta}$ (δ represents the $\Delta\rho_v$ in formula (8)). The parameters in the coupling theory can be calculated by molecular dynamics simulations: $E^0 = 236.036\text{GPa}$, $\nu^0 = 0.267$, $\eta = 0.0728$, $\eta_E = -0.9571$ ^[9].

2.2. The coupling effect of the planar electrolyte

In this section, a planar electrolyte is selected to study the coupling effect, as shown in Fig.1.

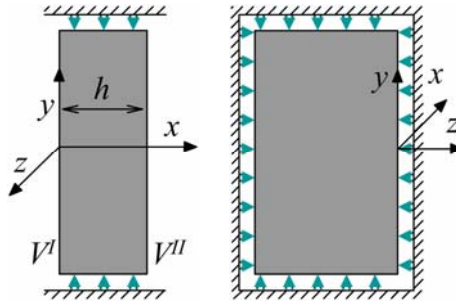


Figure 1. Schematic of electrolyte membrane

The thickness of the membrane is h , and it is completely fixed along y and z directions. The displacement boundary conditions are:

$$u_1 = u(x), u_2 = u_3 = 0 \quad (10)$$

where, $x = x/h$, and the range of values allowed for it is $0 : 1$. The strain tensors are:

$$\varepsilon_{ij}(x_1) = du(x_1)/dx_1 \delta_{ij} \quad (11)$$

Stress tensor can be obtained:

$$\sigma_{11}(x_1) = K(1-\nu^0) \left(\varepsilon_{11}(x_1) - (1+\nu^0)/(1-\nu^0) \eta \Delta\rho_v(x_1) - (1+\nu^0)/(1-\nu^0) \varepsilon^c \right) \quad (12)$$

$$\sigma_{22}(x_1) = \sigma_{33}(x_1) = K\nu^0 \left(\varepsilon_{11}(x_1) - (1+\nu^0)/\nu^0 \eta \Delta\rho_v(x_1) - (1+\nu^0)/\nu^0 \varepsilon^c \right) \quad (13)$$

where $K = K_0(1 + \eta_E \Delta\rho_\alpha)$, and ε^c represents constant strain. Here, pressure is low and no shearing strain exists, so σ_{11} can be assumed zero. According to formula (12), $\varepsilon_{11}(x_1)$ can be obtained:

$$\varepsilon_{11}(x_1) = (1+\nu^0)/(1-\nu^0) \varepsilon^c + (1+\nu^0)/(1-\nu^0) \eta \Delta\rho_v(x_1) \quad (14)$$

Then, the stress tensors can be rewritten as:

$$\sigma_{22} = \sigma_{33} = -\bar{E} \eta \Delta\rho_v(x_1) \left(1 + \eta_E / \eta \varepsilon^c + \eta_E \Delta\rho_v(x_1) \right) \quad (15)$$

where $\bar{E} = E^0 / (1 - \nu^0)$. Bringing formula (15) into (9), we can obtain:

$$\tau_v(x_1) = \bar{E} \left\{ P_0 + P_1 \Delta \rho_v(x_1) + P_2 (\Delta \rho_v(x_1))^2 + P_3 (\Delta \rho_v(x_1))^3 \right\} \quad (16)$$

where:

$$\begin{cases} P_0 = 2\eta\varepsilon^c + 3\eta(\varepsilon^c)^2 + \eta_E(\varepsilon^c)^2, & P_1 = 2\eta^2(1 + 3\varepsilon^c) + \eta\eta_E\varepsilon^c(3\varepsilon^c + 2) \\ P_2 = \eta^2(6\eta_E\varepsilon^c + 3\eta + \eta_E), & P_3 = 3\eta^3\eta_E \end{cases} \quad (17)$$

Besides, the oxygen partial pressure is $\log(P_{O_2}(x=0)/P_{O_2}(x=1)) = -20$, and the chemical boundary conditions can be obtained based on experimental datas^[10]: $\delta(x=0) = 0.1407$, $\delta(x=1) = 0$. Until now, all necessary parameters are obtained: $E^0 = 236.036\text{GPa}$, $\Delta\rho_v(0) = 0.1407$, $\rho_0 = 0.1$, $\eta = 0.0728$, $\eta_E = -0.9571$, $\nu^0 = 0.267$.

3. Description of the multi-scale method

Here, the multi-scale method is defined a combined method of MD simulation with finite element method (FEM). As illustrated in Fig.2.(1), the center-cracked specimen can be decomposed into three parts: in the far field, it is governed by the linear elastic fracture mechanics, at the crack tip, the region is modeled by MD simulation, and the between is called transition region^[11].

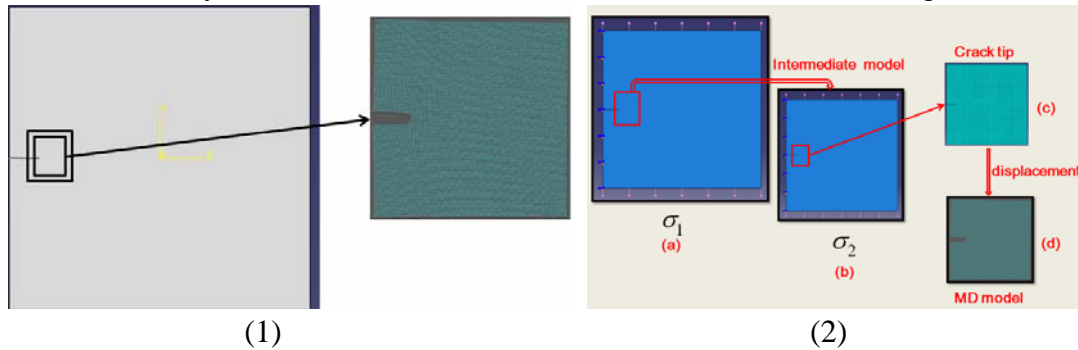


Figure 2. Illustration of the multi-scale model

As seen in Fig.2.(2), an intermediate model is introduced, its size is far smaller than the initial model. During the calculation process, the stress intensity factor (SIF) K_I of the initial model is calculated firstly by FEM. Then the external load σ_2 for the intermediate model can be computed with the same K_I . For the intermediate model, the element size around crack tip is controlled as the same as the lattice constant of CeO_2 , as seen in Fig.2.(2) (c). After the second FEM calculation is completed, the displacements of boundary nodes can be obtained. And then, these displacements are applied to the MD model as boundary conditions for MD simulation. In MD simulation, NPT ensemble is selected, temperature is controlled at 1100K, time step is 1fs (1e-15s), and the in-home potential is used^[9].

4. Simulated results and discussion

The electrolyte membrane with a crack is presented in Fig.3.(a), the length of the crack is 0.04mm,

with the thickness of membrane is 2mm. When the model is loaded, the vacancy concentration near crack tip will be influenced significantly by the high stress field, the interesting phenomenon is called local stress effect.

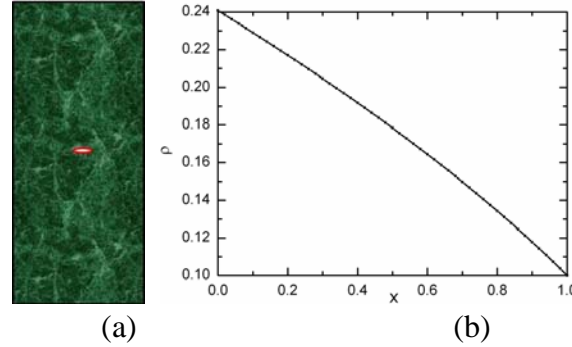


Figure 3. (a) Cross-section of the electrolyte membrane with crack

(b) Distribution of concentration of oxygen vacancy when no local stress effect is considered

Because the stress field is just affected by oxygen vacancy, so only oxygen vacancy is considered here for studying the local stress effect. For comparison, the coupling field without local stress effect is investigated firstly. The diffusion equation of oxygen vacancy is^[18]:

$$J = -D\nabla\rho - (V_m\rho D)/(RT)\nabla\tau \quad (18)$$

Based on the deduction in section 2.2, the diffusion potential τ can be described as:

$$\tau = 3\bar{E}\eta^3\eta_E\Delta\rho^3 + (\bar{E}\eta^2\eta_E + 3\eta^3\bar{E})\Delta\rho^2 + 2\bar{E}\eta^2\Delta\rho \quad (19)$$

Where, $\bar{E} = E^0/(1-\nu^0)$. Equation (19) is plugged into equation (18), the diffusion equation can be obtained:

$$\hat{J} = -\frac{d\rho}{dx} - \frac{V_m\rho}{RT} \left\{ 9\bar{E}\eta^3\eta_E\rho^2 + (2\bar{E}\eta^2\eta_E + 6\eta^3\bar{E} - 18\eta^3\eta_E\rho_0\bar{E})\rho \right\} \frac{d\rho}{dx} + \frac{2\bar{E}V_m\rho}{RT} \left[(\eta^2\eta_E + 3\eta^3)\rho_0 - \eta^2 \right] \frac{d\rho}{dx} \quad (20)$$

where, $\hat{J} = (Jh)/D$, $x = x/h$, h is the thickness of the membrane. The implicit solution can be given out by integrating the equation with chemical boundary conditions:

$$\rho^4 + 2.8751\rho^3 - 6.8512\rho^2 - 1.1028\rho + 0.6189 - 0.4431x = 0 \quad (21)$$

The numerical solution can be calculated by programing the equation, the result is shown in Fig.3.(b).

In order to study the local stress effect, the stress field of the crack-tip (where $\theta = 0$) is applied to the region around the crack tip directly. After the external stress (σ_c) is applied, the stress tensor near the crack tip ($\theta = 0$) can be described as:

$$\begin{aligned}\sigma_{11} &= \frac{K_I}{\sqrt{2\pi}} x^{-1/2} = \frac{K_I}{\sqrt{2\pi h}} x^{-1/2} \\ \sigma_{22} &= -\bar{E}\eta\Delta\rho + \frac{K_I}{\sqrt{2\pi}} x^{-1/2} \\ &= -\bar{E}\eta\Delta\rho + \frac{K_I}{\sqrt{2\pi h}} \left(\frac{x}{h}\right)^{-1/2} = -\bar{E}\eta\Delta\rho + \frac{K_I}{\sqrt{2\pi h}} x^{-1/2}\end{aligned}\quad (22)$$

Where, x is normalized. Similarly, τ can be deduced according to formula (9):

$$\begin{aligned}\tau &= 3\bar{E}\eta^3\eta_E\Delta\rho^3 + \left[\bar{E}\eta^2(\eta_E + 3\eta) + 3\eta^2\eta_E\sigma_c \frac{3\nu-1}{1-\nu} \right] \Delta\rho^2 \\ &+ \left[\frac{3\eta\eta_E}{\bar{E}}\sigma_c^2 + \eta\sigma_c(3\eta + \eta_E) \frac{3\nu-1}{1-\nu} + 2\bar{E}\eta^2 \right] \Delta\rho \\ &+ \frac{1}{\bar{E}}(3\eta + \eta_E)\sigma_c^2 - 2\eta\sigma_c.\end{aligned}\quad (23)$$

For convenience,

$$\begin{aligned}A &= 3\bar{E}\eta^3\eta_E, B = \bar{E}\eta^2(\eta_E + 3\eta) + 3\eta^2\eta_E\sigma_c \frac{3\nu-1}{1-\nu} \\ C &= \frac{3\eta\eta_E}{\bar{E}}\sigma_c^2 + \eta\sigma_c(\eta_E + 3\eta) \frac{3\nu-1}{1-\nu} + 2\bar{E}\eta^2 \\ D &= \frac{1}{\bar{E}}(3\eta + \eta_E)\sigma_c^2 - 2\eta\sigma_c.\end{aligned}\quad (24)$$

Formula (24) is plugged into equation (18), we can obtain:

$$\begin{aligned}\hat{J} &= -\frac{d\rho}{dx} - \frac{V_m\rho}{RT} \left\{ 3A\rho^2 + (2B - 6A\rho_0)\rho + (3A\rho_0^2 - 2B\rho_0 + C) \right\} \frac{d\rho}{dx} \\ &= -\left\{ A'\rho^3 + B'\rho^2 + C'\rho + 1 \right\} \frac{d\rho}{dx}\end{aligned}\quad (25)$$

where,

$$A' = 3V_m/(RT)A, B' = (2B - 6A\rho_0)V_m/(RT), C' = (3A\rho_0^2 - 2B\rho_0 + C)V_m/(RT)\quad (26)$$

By integrating equation (25), the implicit solution can be obtained:

$$3A'\rho^4 + 4B'\rho^3 + 6C'\rho^2 + 12\rho = -12\hat{J} + M\quad (27)$$

where M is a arbitrary constant generated during integration.

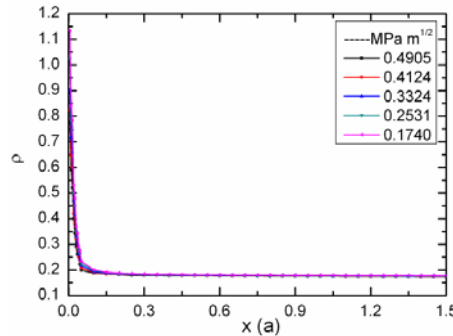


Figure 4. Distribution of concentration of oxygen vacancy near crack tip when stress field of crack tip is applied

As for $\sigma_c = K_I / \sqrt{2\pi x}$, singularity exists at $x=0$. In order to obtain vacancy concentration at crack tip, the K_I is given firstly, and the effective scope of the local stress effect is seted as $1.5a$, where $a=0.02\text{mm}$ is half the length of the crack. Then the value at $x=1.5a$ is calculated, as seen in Fig.4, the value is compared to the corresponding value in Fig.3, it can be found that the difference between the two results is no more than 1%. So the value at $x=1.5a$ is selected as the initial value for the calculation. Then the value at crack tip can be calculated through multiple numerical iteration. The results are plotted in Fig.4. According to the results, it can be observed that the range of values of $\rho(x \approx 0)$ is $0.75 : 1.2$, the range of δ is $0.65 : 1.1(\rho(x \approx 0) - \rho_0)$.

Based on the chemical formula of non-stoichiometric GDC ($\text{Ce}_{0.8-x}^{4+}\text{Ce}_x^{3+}\text{Gd}_{0.2}^{3+}\text{O}_{1.9-\delta}^{2-}$), it can be concluded that the value of δ at crack tip is 0.4 when the local stress effect is considered. The corresponding chemical formula of GDC is $\text{Ce}_{0.8}^{3+}\text{Gd}_{0.2}^{3+}\text{O}_{1.5}^{2-}$. After the multi-scale simulations is completed, the fracture toughness is $0.5142\text{MPa}\sqrt{\text{m}}$. Compared to the fracture toughness of $\text{Ce}_{0.8}\text{Gd}_{0.2}\text{O}_{1.9}$ (20GDC) ($0.9493\text{MPa}\sqrt{\text{m}}$), it is reduced by 45.83%. So, in the process of production and application of the material, the local stress effect should be specially focused.

5. Conclusion

In the work, the coupling theory of the electrolyte in the working environment is presented. In order to study the local stress effect, the electrolyte membrane with crack is selected, and the mechanical behavior of the membrane is studied by using a multi-scale method. According to the simulated results, it can be found that when micro crack exists in the electrolyte membrane, the stress at crack tip is much bigger, and the concentration of oxygen vacancy at crack tip is severely affected. Based on the simulated results, the fracture toughness of the model is decreased to $0.5142\text{MPa}\sqrt{\text{m}}$ when the local stress effect is considered in the working condition, it is reduced by 45.83% compared to the uncoupled value ($0.9493\text{MPa}\sqrt{\text{m}}$). So, in the process of production and application of the material, the local stress effect should be specially focused.

Acknowledgements

This work is supported by National Natural Science Foundation of China (10972066), the Foundation of Excellent Youth of Heilongjiang Province, and the Research Fund for the Doctoral Program of Higher Education of China (20122302110020).

References

- [1] P. Datta, P. Majewski, F. Aldinger, Study of gadolinia-doped ceria solid electrolyte surface by XPS. *Mater Charact*, 60 (2009) 138-143.
- [2] J Roa, E Gilioli, F Bissoli, Study of the mechanical properties of CeO_2 layers with the

- nanoindentation technique. *Thin Solid Films*, 518 (2009) 227-232.
- [3] R. Mangalaraja, S. Ananthakumar, K. Uma, Microhardness and fracture toughness of $\text{Ce}_{0.9}\text{Gd}_{0.1}\text{O}_{1.95}$ for manufacturing solid oxide electrolytes. *Mat Sci Eng A-Struct*, 517 (2009) 91-96.
- [4] G.Y. Wang, V.L. Saraf, M.C. Wang, Microstructure and ionic conductivity of alternating multilayer structured Gd-doped ceria and zirconia thin films. *J Mater Sci*, 44 (2009) 2021-2026.
- [5] F. Ye, T. Mori, J. Zou, A structure model of nano-sized domain in Gd-doped ceria. *Solid State Ionics*, 180 (2009) 1414-1420.
- [6] A. Kossoy, Y. Feldman, R Korobko, Influence of Point-Defect Reaction kinetics on the Lattice Parameter of $\text{Ce}_{0.8}\text{Gd}_{0.2}\text{O}_{1.9}$. *Adv Funct Mater*, 19 (2009) 634-641.
- [7] C.H Wu, The role of Eshelby stress in composition-generated and stress-assisted diffusion. *J Mech Phys Solids*, 49 (2001) 1771-1794.
- [8] N. Swaminathan, J. Qu, Y. Sun, An electrochemomechanical theory of defects in ionic solids: Theory. *Philos Mag*, 87 (2007) 1705-1721.
- [9] Z.W. Cui, Y. Sun, Y.J. Chen, Semi-ab initio interionic potential for gadolinia-doped ceria. *Solid State Ionics*, 187 (2011) 8-18.
- [10] P.D Coll, M.D. Lopez, P. Nunez, Reducibility of $\text{Ce}_{1-x}\text{Gd}_x\text{O}_{2-x}$ in prospective working conditions. *J Power Sources*, 173 (2007) 291-297.
- [11] R.H. Tabar, L. Hua, M. Cross, A multi-scale atomistic-continuum modelling of crack propagation in a two-dimensional macroscopic plate. *J Phys-Condens Mat*, 10 (1998) 2375-2387.